Bacterial Contamination from Stormwater Network Inundation and High Tide Flooding

M. M. Carr[1], A. C. Gold[2], A. Harris[3], K. Anarde[3], M. Hino[4], N. Sauers[1], G. Da Silva[1], C. Gamewell[1], and N. G. Nelson[3,5]

[1]Department of Biological and Agricultural Engineering, North Carolina State University, Raleigh, NC.

[2]Environmental Defense Fund, Raleigh, NC.

[3]Department of Civil, Construction, and Environmental Engineering, North Carolina State University, Raleigh, NC.

[4]Department of City and Regional Planning, University of North Carolina - Chapel Hill, Chapel Hill, NC.

[5]Center for Geospatial Analytics, North Carolina State University, Raleigh, NC.

Corresponding author: Natalie Nelson (nnelson4@ncsu.edu)

Key Points:

- Daily observations of *Enterococcus spp.* concentrations in a coastal waterway were similar during perigean and non-perigean tides.
- Tidal inundation of stormwater networks occurred daily, but rainfall runoff produced the greatest bacterial contamination in the waterway.
- High *Enterococcus spp.* concentrations were observed in roadway floodwaters and the receiving waterway during perigean tides.

Abstract

Inundation of coastal stormwater networks by tides is widespread due to sea-level rise (SLR). The water quality risks posed by tidal water rising up through stormwater infrastructure (pipes and catch basins), out onto roadways, and back out to receiving water bodies is unknown, but may be substantial given that stormwater networks are a known source of fecal contamination. In this study, we (1) documented temporal variation in concentrations of Enterococcus spp. (ENT), the fecal indicator bacteria standard for marine waters, in a coastal waterway over a two-month period and more intensively during two perigean tide periods, (2) measured ENT concentrations in roadway floodwaters during tidal floods, and (3) explained variation in ENT concentrations as a function of tidal inundation, antecedent rainfall, and stormwater infrastructure using a pipe network inundation model and robust linear mixed effect models. We find that ENT concentrations in the receiving water body vary as a function of tidal stage and antecedent rainfall, as well as site-specific characteristics of the stormwater network that drains to the waterbody. Tidal variables significantly explain measured ENT variance in the receiving waterway; however, runoff drove higher ENT concentrations. Samples of floodwaters on roadways during both perigean tide events were limited, but all samples exceed thresholds for safe public use of recreational water. These results indicate that inundation of stormwater networks by tides could pose public health hazards in receiving water bodies and in water pooling on roadways. These health hazards will likely be exacerbated in the future due to continued SLR.

Plain Language Summary

Communities along the US Atlantic Coast have begun to experience the effects of sea-level rise as stormwater drainage pipes, originally designed when sea levels were lower, are now routinely inundated at high tide. We do not know the water quality of the floodwaters or whether flooding affects the quality of the bodies of water receiving the floodwaters. In this study, we collected daily water samples from a tidal creek over a two-month period and tested the samples for *Enterococcus spp.* (ENT), the bacteria used by regulators to assess the safety of marine waters for swimmers and recreators. We also collected water samples during the highest high tides from roadway floodwaters and the adjacent tidal creek as the stormwater pipes drained during outgoing tide. After data collection, we developed statistical models to relate the amount of ENT in the tidal creek to characteristics of the tide, rainfall, and stormwater infrastructure. Rainfall caused greater bacterial contamination in the tidal creek than high tide flooding. However, we observed high ENT concentrations in roadway floodwaters and in the creek during the outgoing tide, leading us to conclude that everyday flooding of underground stormwater pipes at high tide could create hazardous water quality.

1 Introduction

Since 1880, global sea level has risen between 21 and 24 cm, and on the Atlantic Coast of the United States where many coastal communities were built on low-lying land, sea levels have risen at even higher rates (Sweet et al., 2022). For many of these coastal communities, stormwater infrastructure, like subterranean pipe networks, ditches, and catch basins, was built decades ago when sea levels were lower. Now, this rise in sea level has allowed tides to propagate up into stormwater networks and overtop low elevation areas, causing coastal communities to flood in what is referred to as "sunny day flooding" or "high tide flooding". Regular tidal inundation of stormwater networks has become widespread in coastal areas (Gold

65 et al., 2022), and persistent increases in sea level rise (SLR) are projected to increase the
66 frequency and magnitude of high tide flooding nationally (Sweet et al., 2022).

67 As tidal floods increase in frequency and magnitude, aging and faulty stormwater
68 infrastructure may pose a public health risk by creating water quality hazards (Allen et al., 2019).
69 Stormwater networks can act as reservoirs for fecal contaminants, as exfiltrated sewage (Hart et
70 al., 2020; Olds et al., 2018), biofilms (Burkhart, 2013), or septic leachate (Converse et al., 2011)
71 can be present within the network. Frequent inundation by tidal waters could transport fecal
72 contaminants from stormwater networks to roadways during incoming or "flood" tides, and flush
73 pollutants into coastal waters during outgoing or "ebb" tides. Other factors, like stormwater
74 runoff (Shen et al., 2019; Gold et al., 2023) and high groundwater tables (Befus et al., 2023;
75 Habel et al., 2020), can compound with tides and reduce the volume capacity of stormwater
76 networks, leading to more extensive or frequent flooding of coastal communities.

77 Increased attention has been dedicated to tidal inundation as a transport mechanism of
78 fecal contamination through stormwater infrastructure inundation (Hart et al., 2020; Price et al.,
79 2021), overtopping of coastal infrastructure (Macías-Tapia et al., 2021, 2023), and groundwater
80 inundation (McKenzie et al., 2021). Hart et al. (2020) measured human-specific microbial source
81 tracking markers in a municipal separate stormwater system (MS4) in Beaufort, NC, during
82 compound high tide and storm conditions, proposing that diluted sewage could be present in
83 standing water on the roadway when high tide floods occur. This work was continued by Price et
84 al. (2021), who determined that the highest concentrations of fecal indicator bacteria (FIB) in
85 stormwater discharge were present in receding tides during nineteen sampling events
86 encompassing both storm and ambient conditions. Macías-Tapia et al. (2021, 2023) reported
87 consistent exceedances of *Enterococcus spp.* (ENT), a fecal indicator bacteria used in marine and
88 beach water quality standards from the U.S. Environmental Protection Agency (EPA,
89 Recreational Water Quality Criteria, 2012), in tidal floodwaters and receiving waters of the
90 Lafayette River in Norfolk, VA during five annual perigean spring tide flooding events between
91 2017 and 2021. This work determined that loads varied between floods but no relationship
92 between ENT abundance and floodwater extent could be determined (Macías-Tapia et al., 2023).
93 Lastly, McKenzie et al. (2021) monitored coastal and canal groundwater and surface water and
94 storm drains during high tide events and reported the presence of wastewater discharge in the
95 collected samples through measurement of radon and wastewater tracers. Combined, these
96 studies provide insight into the potential role of tidal flooding as a mechanism for fecal
97 contamination in coastal waters. However, to understand how stormwater network inundation by
98 tides is a driver of coastal fecal contamination, longitudinal data are needed to understand how
99 contaminant dynamics vary across locations, over time, and with flood events of different drivers
100 (e.g., tides and rainfall) and magnitudes.

101 In this study, we assessed the potential for fecal contamination in an urban, coastal
102 waterway that experiences tidal floods and daily inundation of its underground stormwater
103 network by tides. Specifically, our objectives were to (1) document temporal variation in fecal
104 bacteria concentrations in a coastal waterway over multiple flood events and under baseline
105 conditions, (2) measure fecal bacteria concentrations in roadway floodwaters during tidal flood
106 events, and (3) explain variation in bacteria concentrations as a function of tidal inundation,
107 antecedent rainfall, and stormwater infrastructure. Since fecal contaminants are highly variable
108 in space and time (Boehm, 2007), we collected observational data at three locations daily over a
109 two month period, and more intensively during nine tidal cycles coinciding with two perigean

110 tide events (i.e., some of the highest tide events of the year, when the moon is closest to the
111 earth). These measurements, in conjunction with a simplified pipe network model and linear
112 regression, were used to explain variation in bacteria concentrations in the waterway as a
113 function of tidal inundation, antecedent rainfall, and stormwater infrastructure. Water quality
114 samples were also collected from the roadway during tidal floods to provide context for the
115 range of potential human health impacts from stormwater network inundation driven by SLR.

116 **2 Methods**

117 2.1 Site Description

118 Our study site was Beaufort, North Carolina, USA, a small, coastal town established in
119 the 1700s. Beaufort sits on a peninsula between the Newport River and North River (to the west
120 and east, respectively) and north of Taylor's Creek, a tidal channel that empties through an inlet
121 to the Atlantic Ocean. We focused our sampling efforts on Taylor's Creek, which is the receiving
122 waterbody that is adjacent to the downtown area, and on the roadway closest to the waterway
123 Front Street (**Fig 1a**). The tides in Taylor's Creek are semi-diurnal with a tidal range of 0.95 m
124 (NOAA Tides and Currents Station ID: 8656483, located in Beaufort, NC). In 2016, Taylor's
125 Creek was listed as a 303(d) impaired waterway for ENT by the North Carolina Division of
126 Environmental Quality, but was later delisted in 2022 after stormwater network improvements
127 (NCDEQ, 2022 North Carolina 303(d) List, 2023).

128 Much of the shoreline in the downtown area is armored with bulkheads, which protects
129 roadways and other low-lying areas from high water levels in Taylor's Creek. Stormwater is
130 conveyed to Taylor's Creek via a MS4, consisting of subterranean pipes and several outfalls
131 within our sampling area (**Fig 1b**). Roadway flooding is monitored on Front Street by water level
132 gauges located within the stormwater network, as well as pole-mounted cameras (Gold et al.,
133 2023). These data have shown that tides inundate the stormwater network on a daily basis;
134 during perigean tide events, water can rise all the way up through the network and result in
135 flooding of roadways. During regular tides, flooding can still occur due to the compounding
136 effects of rainfall, as there is limited capacity for pipes to convey even small amounts of rainfall
137 as a result of tidal water volumes occupying some of the capacity (Gold et al., 2023). In 2023,
138 the Town of Beaufort installed a backflow prevention device at one outfall, which has reduced
139 tidal inundation along parts of the stormwater network. But during our study period, which
140 spanned June 6 to August 2, 2022, the stormwater network contained no backflow devices,
141 which allowed for regular inundation with the tide (as in Gold et al., 2023).

142 Two perigean tide events occurred during the study period: one spanning June 12-17 and
143 the other July 11-16, 2022 (University of North Carolina - Chapel Hill, NC King Tides Project,
144 2022). During the highest-high tides associated with these events, tidal waters propagated up
145 through the stormwater network and produced minor roadway flooding nine times. No
146 concomitant rainfall occurred during the highest-high tides of the two perigean tide events, so
147 that the floodwaters were produced from tidal influence only. Rainfall occurred during the higher
148 low tide on July 15, 2022, and produced a compound flood event. Compound flood events occur
149 when a rainfall event coincides with reduced stormwater network capacity from tidal inundation.
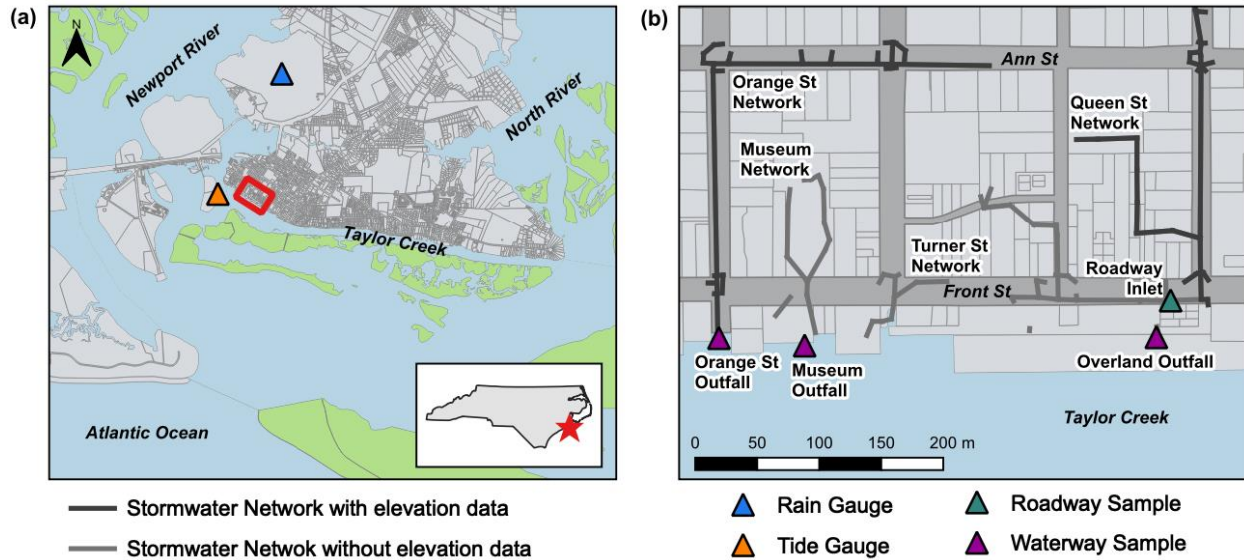
150

Figure 1. Study maps of Beaufort, NC, USA (**a**) and the four stormwater networks in downtown
Beaufort, NC, USA (b). Thin gray lines delineate land parcels. In (**b**), thick gray lines show the
underground stormwater pipe network, with the shade of gray indicating whether there was
elevation data available (dark and light for networks with known and unknown elevation,
respectively). Waterway samples were collected from Taylor's Creek at three locations (purple
triangles) within 10 meters of stormwater outfalls. Roadway flood samples were collected
directly above a single stormwater catchment grate in the Queen Street network (teal triangle).
The NOAA tide gauge (orange triangle), which informed sampling times and tidal variables, is
located across Taylor's Creek approximately 300 m from the Orange Street Outfall sampling
location. The rain gauge (blue triangle) is located north of the study site.

2.2 Data Collection

Water quality samples were collected for enumeration of ENT concentrations. Collection
occurred at three waterway locations in Taylor's Creek (**Fig 1b**). The "Overland Outfall"
sampling location is near a bulkhead spillway that conveys stormwater runoff from a parking lot
and is not connected to the subterranean pipe network. The overland outfall is relatively high in
elevation and was not observed to be inundated during our study period. The "Museum Outfall"
drains a relatively small area (**Fig 1b**), including a parking lot around a museum and catch basins
on Front Street. The "Orange Street Outfall" sampling location was located 2 m from the Orange
Street outfall, which drains a relatively large area, including a residential street and catch basins
on Front Street and Ann Street (**Fig 1b**). The Orange Street Outfall sampling location was added
on June 14, 2022, a week after sampling was initiated at the Overland Outfall and the Museum
Outfall locations. Outfall elevations were only available for the Orange Street Outfall, which is
positioned at -0.74 m NAVD88 or -0.30 m Mean Higher-High Water (MHHW). The MHHW
datum is the mean of the highest diurnal tide, and is useful for identifying extremes in tidal
heights. Water levels greater than the 0 m MHHW datum are deviations of tidal heights above
the average high tide. At this elevation, the Orange Street Outfall is inundated by tides on a daily
basis.

Collection of water samples in Taylor's Creek, proximate to the three outfall locations
described above, occurred daily over a period of two months. This allowed for characterization

180 of water quality during both baseline conditions and perigean tides. Baseline sampling of ENT (n
181 = 163) occurred daily between 8:00-9:00 AM Eastern Time to prevent ENT levels from being
182 affected by UV inactivation from direct sunlight, which peaks around midday. Given the two-
183 month long sampling period, the daily samples also captured every tidal stage (low, rising, high,
184 falling tide). Perigean tide sampling of ENT (n = 89) occurred during nine roadway flood events
185 spanning June 12-16 and July 11-15, 2022 (as noted above, the perigean tides extended into the
186 morning of the next day, from June 12-17 and July 11-16, 2022). During these flood events, we
187 increased the sampling frequency to include measurements at high tide, ebb tide (approximately
188 halfway between high and low tide), and low tide, with measurement times scheduled based on
189 predicted water levels at the nearby NOAA Tides and Currents Station (NOAA, ID 8656483; Fig
190 1). This sampling frequency was selected to capture the change in water quality conditions from
191 the maximum stormwater inundation (at highest high tide) and during the draining of the
192 stormwater networks (during the ebb tide and at the highest low tide). During these floods, we
193 also sampled roadway floodwaters at a stormwater grate in the Queen Street stormwater network
194 (n = 10). We define a roadway flood as any amount of water above the elevation of the
195 stormwater grate.

196   Sterile, pre-rinsed 100 mL FalconTubes (polypropylene material) were used to collect
197 100 mL water samples 0.5-1 m below the water surface at the three waterway sampling
198 locations, and at surface depth in the floodwaters on the roadway. After collection, samples were
199 stored in a cooler at 4°C during transport to the laboratory. Water samples were processed in
200 duplicate for ENT following the IDEXX Enterolert standard protocol with the Quanti-tray 2000
201 (IDEXX, ASTM Method #D6503-99). The IDEXX assay requires a 100 mL sample volume, and
202 due to salinity content of the water samples, 10 mL of water sample was mixed with 90 mL of
203 deionized water. Samples were provided the IDEXX media and incubated for 24 hours at 41°C ±
204 0.5°C. ENT concentrations were estimated using a most-probable number (MPN) technique
205 based on the number of large and small wells of the quanti-trays fluorescing under UV light,
206 with a modified laboratory detection range of 10-24,196 most probable number ENT per 100 mL
207 water (MPN 100 mL^{-1}) due to sample dilution. During sample collection and laboratory analysis,
208 field blanks (n = 27) and laboratory blanks (n = 30) were also collected and processed for quality
209 assurance and quality control purposes.

210   ENT concentrations were classified as above or below the EPA's single sample
211 maximum threshold concentration for safe public use of recreational waters of 104 MPN 100
212 mL^{-1} (EPA, Recreational Water Quality Criteria, 2012). This EPA standard is for recreational use
213 of marine waters, meaning it directly applies to water samples collected from Taylor's Creek, but
214 does not directly apply to the assessment of roadway floodwaters, which are not recreational
215 waters. Given that a standard does not exist for floodwaters of any kind – whether storm or
216 tidally driven – but that pedestrians can still make contact with floodwaters, we consider the
217 EPA's recreational standard here as a benchmark for comparison of water quality measurements
218 collected from the roadway during the tidal floods.

219 2.3 Pipe Network Inundation Model

220   A pipe network inundation model of Front Street was used to characterize the extent of
221 tidal inundation within the stormwater network during the measured flood events. Generally, a
222 pipe network inundation model is a "bathtub" approach that simulates flooding by gradually
223 filling subterranean pipes based on the elevation of the pipe relative to the level of the waterbody

224 (Strauss et al., 2012). The pipe network inundation model used in this study was generated using
225 the *bathtub* R package (Gold et al., 2022) and is the same model used by Gold et al. (2022) for
226 Beaufort, NC. This model was developed using elevations from a 2017 survey, during which
227 some structures were inaccessible. Hence, our pipe network inundation model is incomplete for
228 the Front Street study area, but can be used to estimate stormwater network inundation in two of
229 the studied stormwater pipe systems, specifically the Orange Street and Queen Street pipe
230 networks (Fig. 1b). The percentage of stormwater network inundation was quantified at discrete
231 water levels by averaging the percent fill of surveyed stormwater point structures (e.g., drop
232 inlets and catch basins) on Front Street, specifically the Orange Street network and the northern
233 section of the Queen Street network.

234 2.4 Explanatory Variables used in Linear Regressions

235   We sought to explain measured variation in ENT concentrations within the waterway
236 with both tidal and rainfall factors using robust linear mixed effect regressions. Tidal variables
237 used in the explanatory analysis include tidal height at time of sample collection, time since the
238 last high tide before sample collection, and the height of the last high tide before sample
239 collection. Tidal height at the time of sample collection was taken from the nearby NOAA Tides
240 and Currents gauge (Fig 1a, which has been shown to match well with measured water levels in a
241 stormwater catch basin on Front Street when it is not raining (Gold et al., 2023). The height of
242 the last high tide, and the time since the last high tide, were likewise calculated using the NOAA
243 tide gauge data. We chose to include time since the last high tide before sample collection and
244 the height of the last high tide before sample collection to account for a potential lagged response
245 of ENT concentrations in the waterway as tidal waters recede from the stormwater network,
246 relative to the timing of maximum inundation of the stormwater network.

247   Because Taylor's Creek is a coastal waterway, it receives ENT loads by both direct
248 runoff from stormwater outfalls and fluvial transport through the local watershed. To account for
249 these transport pathways, we considered rainfall factors in the explanatory analysis. Seven
250 rainfall variables were analyzed, all of which correspond to (antecedent) rainfall totals over finite
251 intervals, including rainfall over 3, 6, 12, 24, 36, 48, and 72 hours prior to sample collection (in
252 mm). These variables were calculated using hourly rainfall depths (millimeters) obtained from
253 the Michael J Smith Airport weather station located approximately a mile north of Front Street in
254 Beaufort, NC (North Carolina State Climate Office, station ID: KMRH; **Fig 1a**). The June
255 rainfall total was 50 mm, and only one storm event produced a rainfall depth over 13 mm (or
256 0.51 inches). In contrast, the July rainfall total was 400 mm and 8 storm events produced rainfall
257 depths greater than 13 mm.

258 2.5 Regression Analysis

259   ENT concentrations from the waterway were first logarithmically transformed to account
260 for the exponential range of bacteria counts observed. The relationship between logarithmically
261 transformed ENT concentrations ($\log_{10}$ ENT) and sampling location was then assessed using the
262 Friedman test, which is a hypothesis test for repeated measures. We selected the Friedman test
263 because the daily collection of ENT constitutes a repeated measure and the test does not assume
264 an underlying distribution for the grouped-by-location data. The Friedman test determines
265 whether the median value of a treatment group is significantly different from the median values

266   of the other treatment groups. We assessed significance with an alpha value of 0.05. The
267   Friedman test was calculated using the *stats* R package (R Core Team, 2013).

268   Next, the relationships between $\log_{10}$ ENT, tidal, and rainfall variables were analyzed
269   using robust linear mixed effect models with the *robustlmm* R package (Koller, 2016) for both
270   baseline conditions and during perigean tides that corresponded with roadway flooding (i.e., the
271   nine roadway flood events spanning June 12-16 and July 11-15, 2022). Individual robust linear
272   mixed effect regressions between $\log_{10}$ ENT and each explanatory variable were performed to
273   evaluate pairwise relationships. Models representative of baseline conditions (the "baseline"
274   models) were generated using data from the entire two-month study period, which captured daily
275   stormwater network inundation and multiple rain events. In contrast, models spanning perigean
276   tide conditions (the "perigean tide" models) were generated only using data following
277   stormwater network inundation by the perigean tides that resulted in roadway flooding (i.e.,
278   complete inundation of the stormwater network). We selected robust linear mixed effect models
279   because of the repeated-measures structure of our sampling design and the presence of outliers
280   and non-normal residuals in the $\log_{10}$ ENT data set.

281   Given that the waterway data varies both in space and time, the baseline mixed effect
282   model has the following equation structure:

$$\log_{10} \text{ENT} = \text{Explantory Variable} + (1 \mid \text{Site}) \qquad \text{Equation 1}$$

283   Where "|" denotes that the sampling location, or "Site", is a random effect. The perigean tide
284   model has the equation structure:

$$\log_{10} \text{ENT} = \text{Explantory Variable} + (1 \mid \text{Site})$$
$$+ (1 \mid \text{Perigean Tide} / \text{Categorical Tidal Stage}) \qquad \text{Equation 2}$$

285   Where "Site" and "Perigean Tide" (June or July) are random effects and "Categorical Tidal
286   Stage" (high, ebb, and low tide) is a nested random effect within the "Perigean Tide" random
287   effect. No interaction exists between the "Site" and "Perigean Tide / Categorical Tidal Stage"
288   terms because the sampling design produced a crossed-data structure between sampling period
289   and site. The tidal and rainfall explanatory variables are fixed effects and were centered and
290   scaled in the baseline models and perigean tide models. Conditional R^2 (variance explained by
291   random and fixed effects) and marginal R^2 (variance explained by fixed effects or explanatory
292   variables) were calculated for each regression using the *performance* R package (Lüdecke et al.,
293   2021). Results are discussed in terms of their marginal R^2 value since marginal R^2 values only
294   include the effect of the explanatory variable while conditional R^2 values also include the effects
295   of random variables. Additionally, p-values and slopes were calculated to identify significant
296   positive or negative relationships (alpha = 0.05) using the *parameters* R package (Lüdecke et al.,
297   2020). All analyses were performed using R version 4.2.2 (R Core Team, 2022).

3 Results and Discussion

3.1 Tidal stormwater network inundation occurred daily

300   Water level data from within a storm drain on Front Street showed that the Queen Street
301   network was inundated daily over the two month study period at each higher-high tide (n =
302   60/60, Gold et al., 2023). Using the pipe network model, we find that the stormwater network
303   along other areas of Front Street was on average 57% inundated during the higher-high tides (on

304 average 0.16 m MHHW) and 0.6% inundated during the lower-low tides (on average -0.91 m
305 MHHW) during baseline conditions (**Fig 2a-2b**). During the perigean tide events, the average
306 lower low tide and higher high tide elevations were -1.1 and 0.40 m MHHW, respectively, which
307 correspond to modeled stormwater network inundation percentages of 0 and 78% along Front
308 Street, respectively (Fig 2c-2d). During these events, inundation of the stormwater network
309 extended inland beyond Front Street, filling pipes nearly 40% with tidal water (**Fig 2c**).
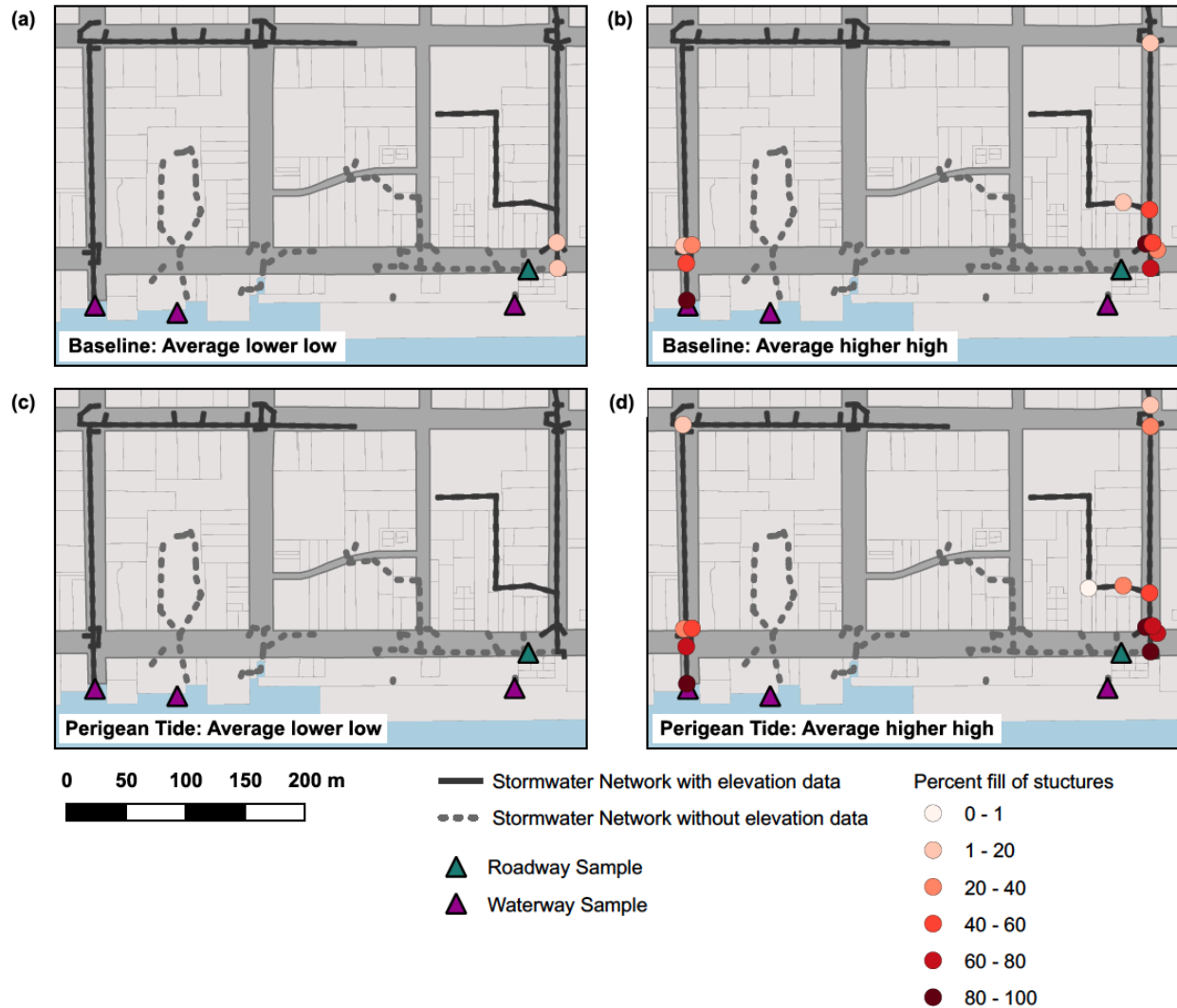

310
311 **Figure 2**. Modeled tidal inundation of two stormwater networks in downtown Beaufort during
312 the study period. The average percent fill of stormwater catchments (attached to subterranean
313 pipes) is shown for lower low tide (**2a**,**c**) and higher high tide (**2b**,**d**) for the baseline data
314 collected from June 6 to August 2, 2022 (**2a**,**b**), and for the perigean tide data collected on June
315 12-17 and July 11-16, 2022 (**2c**,**d**).

316   Our pipe network model only accounts for variation in tidal elevation, as measured by the
317 nearby NOAA tide gauge, and does not consider water level contributions from rainfall runoff,
318 groundwater infiltration into the stormwater network, or pipe hydraulics. Bathtub models, like
319 the pipe network model used here, typically overestimate flooding compared to models that
320 account for pipe hydraulics (e.g., Castrucci & Tahvildari, 2018; Gallien et al., 2014). However,

321 outside of rain events, Gold et al. (2023) showed that water levels in the Queen Street network
322 track well with water levels measured at the NOAA tides gauge during baseline conditions,
323 indicating that contributions from groundwater infiltration into the stormwater network are likely
324 small for the pipe network. During rainfall events, the pipe network model is an underestimate of
325 actual inundation.

326 While the network inundation model does not consider non-tidal forcing and pipe
327 hydraulics, it can be used to estimate where inundation was relatively high and low across the
328 network due to tidal forcing alone. In particular, the network inundation estimates highlight that
329 total network inundation and roadway flooding were most likely to occur in and along the Queen
330 Street network. The pipe network model also reveals that the Orange Street network experienced
331 daily and major inundation, but to a lesser extent than the Queen Street network. Due to the inlet
332 and outfall elevations not being surveyed, we are unable to assess the frequency at which the
333 museum network was inundated.

334 3.2 Daily waterway ENT concentrations differed between sampling locations

335 ENT was detected in 73% of daily, or baseline, samples (n = 241/330) with
336 concentrations ranging from 10 to 5,298 MPN 100 mL^{-1} (**Fig 3**). ENT measurements exceeded
337 the single sample maximum threshold concentration for safe public use of recreational waters
338 (104 MPN 100 mL^{-1}) in 16% of the daily samples, indicating recurring but infrequent levels of
339 unsafe fecal contamination in the waterway during the two month summer sampling period.
340 Similar daily ENT concentrations in the waterway were observed between non-perigean and
341 perigean tide periods. Hence, while perigean tide events lead to increased stormwater network
342 inundation (**Fig 2d**), they did not necessarily result in increased ENT loading within the
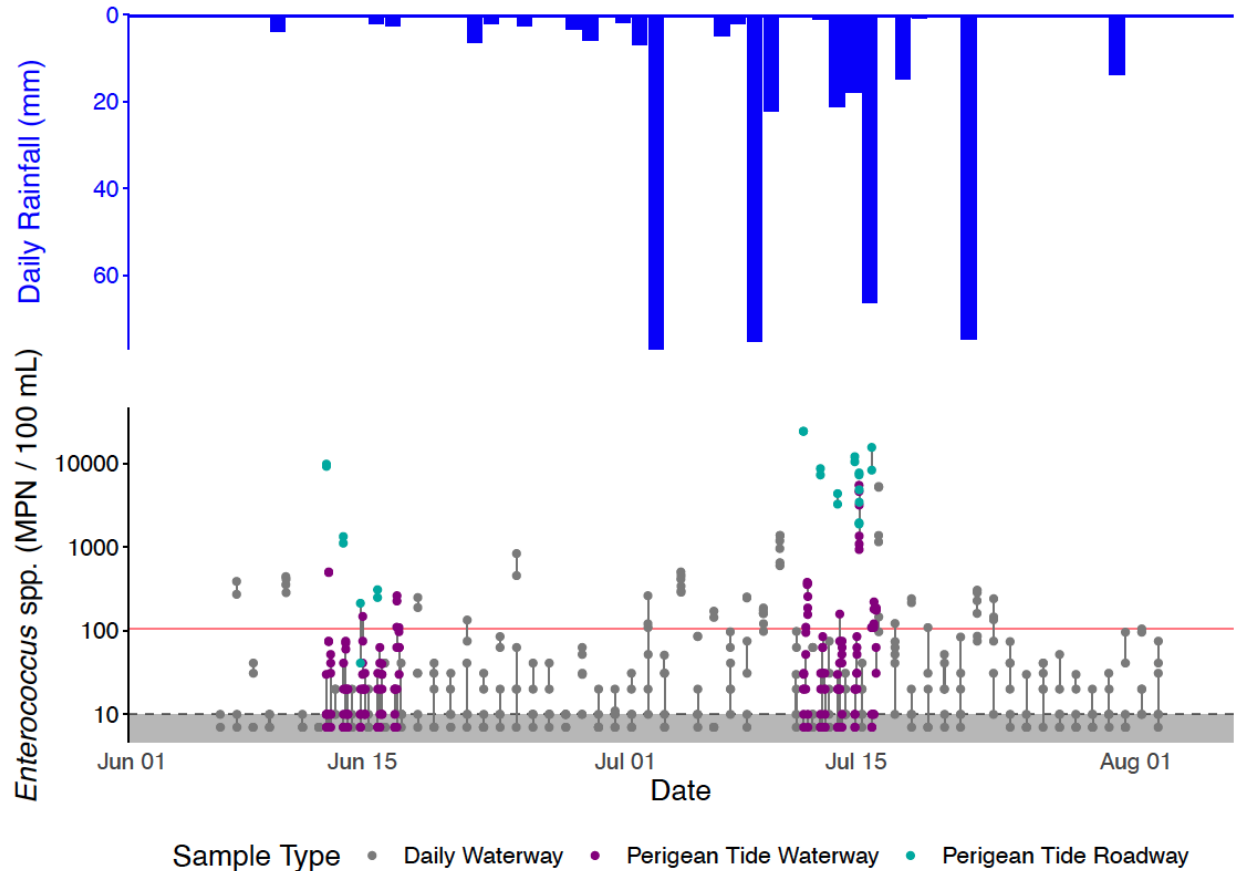343 waterway.

344

Figure 3. Daily rainfall (top) and ENT concentrations (bottom) during flood (perigean tide) and
baseline conditions throughout June and July 2022. The red line represents the EPA's single
sample maximum threshold concentration for safe public use (104 MPN 100 mL^{-1}), and the
grayed area represents the minimum detection limit (below 10 MPN 100 mL^{-1} for samples
diluted 10:1). Gray and purple points correspond to measurements taken in Taylor's Creek
during basline and flood conditions at the three sampling locations, respectively, while teal
points correspond to measurements taken from roadway floodwaters above a single stormwater
catchment grate in the Queen Street network. Samples were processed in duplicate, and duplicate
measurements are connected by vertical lines to visualize uncertainty.

We found there were significant differences in ENT concentrations by sampling location
(alpha < 0.05). During baseline conditions, the Orange Street Outfall had the highest median
concentration of ENT in the waterway (31 MPN 100 mL^{-1}) while the sampling locations near the
Museum and Overland Outfalls showed lower median ENT concentrations (both 10 MPN 100
mL^{-1}, which corresponds to the minimum detection limit). Inter-site variability between outfall
sampling locations was also noted by Price et al. (2021), who posited that site-specific
infrastructure can cause localized water quality dynamics.

For June, the median ENT concentration was 20 MPN 100 mL^{-1} and had an interquartile
range of <10 to 23 MPN 100 mL^{-1} while the July median concentration was 41 MPN 100 mL^{-1}
and had an interqurtile range of 10 to 86 MPN 100 mL^{-1}. Rainfall occurred more frequently in
July than in June. Periods of increased rainfall are known to correspond with increased FIB

365 concentrations in waterways due to runoff-driven contamination and elevated surficial
366 groundwater elevations, which can also lead to greater sewage exfiltration (Secru et al., 2011).
367 The modeling results of baseline conditions, which show significant relationships between $\log_{10}$
368 ENT and prior 3, 6, 12, 24, 48, and 72 hour rainfall totals (alpha < 0.05), reflect the influence of
369 rainfall on the variance of bacterial concentrations (**Table 1**).

370 **Table 1**. Linear regression models of baseline conditions (top) and perigean tide conditions
371 (bottom) between $\log_{10}$-transformed ENT concentrations ($\log_{10}$ MPN) and tidal or rainfall
372 factors.

Baseline Conditions (n =163 observations); random effect = sampling location					
Explanatory Variables (fixed effect)	Conditional R^2 (full model)	Marginal R^2 (fixed effects)	p-value (alpha)	Coefficient	Standard Error
Tidal Factors					
Tidal Height	0.17	0.06	< 0.05	-0.15	0.03
Time to Last High Tide	0.16	0.04	< 0.05	0.12	0.03
Height of Last High Tide	0.12	0.01	0.07	-0.06	0.03
Rainfall Factors					
Prior 3-hour rainfall	0.23	0.11	< 0.05	0.21	0.03
Prior 6-hour rainfall	0.27	0.14	< 0.05	0.24	0.03
Prior 12-hour rainfall	0.39	0.27	< 0.05	0.34	0.03
Prior 24-hour rainfall	0.46	0.35	< 0.05	0.38	0.03
Prior 48-hour rainfall	0.40	0.31	< 0.05	0.36	0.03
Prior 72-hour rainfall	0.30	0.21	< 0.05	0.29	0.03
Perigean Tide Conditions (n = 89); random effects = sampling location, categorical tidal stage, flood					
Explanatory Variables (fixed effect)	Conditional R^2 (full model)	Marginal R^2 (fixed effects)	p-value (alpha)	Coefficient	Standard Error
Tidal Factors					
Tidal Height	0.34	0.20	< 0.05	-0.28	0.07
Time to Last High Tide	0.34	0.13	< 0.05	0.22	0.11
Height of Last High Tide	0.39	0.01	0.21	-0.05	0.04
Rainfall Factors					
Prior 3-hour rainfall	0.42	0	0.78	-0.01	0.05
Prior 6-hour rainfall	0.37	0	0.52	0.03	0.05
Prior 12-hour rainfall	0.38	0	0.56	0.03	0.05

373   3.3 Roadway floodwaters had consistently high ENT concentrations

374   We visually observed nine minor floods localized to the Queen Street stormwater
375   network, and no roadway flooding via the Orange Street and Museum stormwater networks
376   during perigean tides. The presence of flooding was corroborated by the storm drain water level
377   measurements and the pipe network model. The floodwater samples exceeded the EPA's single
378   sample maximum threshold concentration for safe public use (104 MPN 100 mL^{-1}) for 8 of the 9
379   high tide flood events, in many cases by an order of magnitude (**Fig 3**). These ENT
380   concentrations are comparable to the concentrations reported by Macías-Tapia et al. (2021, 2023)
381   in Norfolk, VA in 2017, when 95% of the ENT samples exceeded the single sample maximum
382   threshold concentration and ENT concentrations ranged from 30 to >24,000 MPN 100 mL^{-1}.

383   In June, the median floodwater concentration was 710 MPN 100 mL^{-1} and concentrations
384   ranged from 41 to 9,804 MPN 100 mL^{-1} (**Fig 3**). By comparison, in July, the median floodwater
385   concentration was 9,563 MPN 100 mL^{-1} and concentrations ranged from 1,882 to >24,196 MPN
386   100 mL^{-1}. The perigean high tide elevations were similar between June and July (0.35-0.51 and
387   0.34-0.45 m MHHW, respectively), as was the modeled inundation percentages at higher high
388   tide (75-87 and 73-81%), so we hypothesize that differences in concentrations stem from
389   antecedent rainfall factors. These findings suggest that antecedent rainfall can enhance fecal
390   contamination in roadway floodwaters during high tide flood events. But, importantly, given that
391   the June floodwaters were still more than 6 times higher than the EPA standard in the absence of
392   rainfall, complete inundation of stormwater networks by tides in drier conditions can create
393   concerning water quality conditions in roadway floodwaters.

394   The sources of fecal bacteria in the roadway floodwater samples are unknown. We
395   believe the primary fecal bacteria sources during the high tide floods sampled were within the
396   stormwater network. We observed fecal contamination in roadway floodwaters in the absence of
397   rain, due solely to stormwater network inundation by tides, indicating a source from either
398   Taylor's Creek or the stormwater network. However, water quality samples collected near
399   stormwater outfalls in Taylor's Creek did not have similarly high concentrations (**Fig 3**), so
400   Taylor's Creek is likely not a primary source of fecal bacteria to the floodwaters. Lastly, the
401   majority of the roadway floods were small and confined to puddles around the storm drains (**Fig
402   4**), indicating that the floodwaters likely did not flush fecal matter from the land surface.
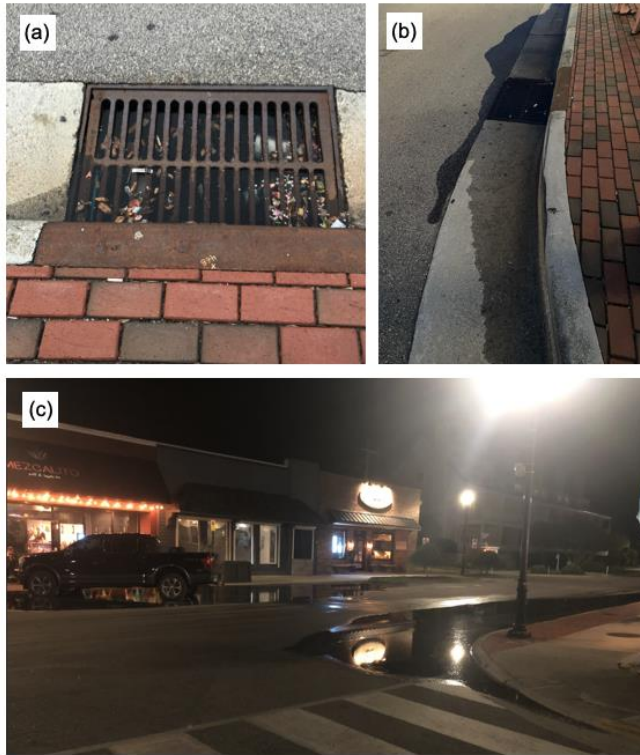
403

Figure 4. Tidal flooding at high tide on June 12, 2022 at 7:18PM (**a**), June 14, 2022 at 8:52PM
(**b**), and June 15, 2022 at 9:51PM (**c**). We define a roadway flood as any amount of water above
the elevation of the stormwater grate.

Because tidal inundation of stormwater networks can impede drainage of stormwater
runoff, it may be that stormwater runoff with high ENT concentrations remain in the network as
stagnant water for extended periods of time, potentially spilling into the roadway during the next
high tide. Additional sources of fecal bacteria in the stormwater network could include
exfiltrated sewage (Hart et al., 2020), and local environmental reservoirs of bacteria in biofilms
and sediment (Burkhart, 2013). Importantly, since the majority of our measurements were
collected from roadway floods with small overland extents, we are unable to assess whether high
ENT concentrations would persist during more extensive floods, or if more extensive floods may
dilute ENT concentrations instead, as proposed by Lewis et al. (2013).

3.4 Highest median ENT concentrations occurred during ebb tide

To capture the water quality of receding tidal waters from the stormwater network during
the perigean tide events, ENT measurements were collected at multiple tidal stages in the
waterway: at high tide, ebb tide, and low tide (**Fig 5**). We observed a general trend that ENT
concentrations increased from high tide to ebb tide and decreased from ebb tide to low tide. This
trend has been previously reported for Taylor's Creek in Price et al. (2021), who observed that
ENT increased during ebb tide as tidal height decreased and the stormwater network drained. In
this present study, median concentrations at high, ebb, and low tide across both the June and July
perigean tide events were 10, 52, and 30.5 MPN 100 mL^{-1}, respectively (**Fig 5**). Sixty percent (n
= 36/60) of high tide samples had ENT concentrations below the minimum detection limit of 10

426   MPN 100 mL^{-1}. Then, as the tidal waters receded from the stormwater network during ebb tide,
427   ENT concentrations increased. From the linear regression analysis, we found that this trend was
428   reflected in a significant negative relationship (coefficient = -0.28, alpha < 0.05) between tidal
429   height at sample collection and ENT concentrations in the perigean tide models (**Table 1**). This
430   increase in median ENT concentrations from high to ebb tide suggests that receding tides
431   transport ENT from the stormwater network to the waterway. However, we also observe a
432   decrease in median ENT concentrations from ebb to low tide, which suggests that the effect of
433   receded tidal waters on ENT concentrations in the waterway was short lived. This could
434   potentially be explained by flushing or dilution. UV inactivation should not have affected the
435   measured ENT concentrations given that the perigean tide sampling occurred at night during
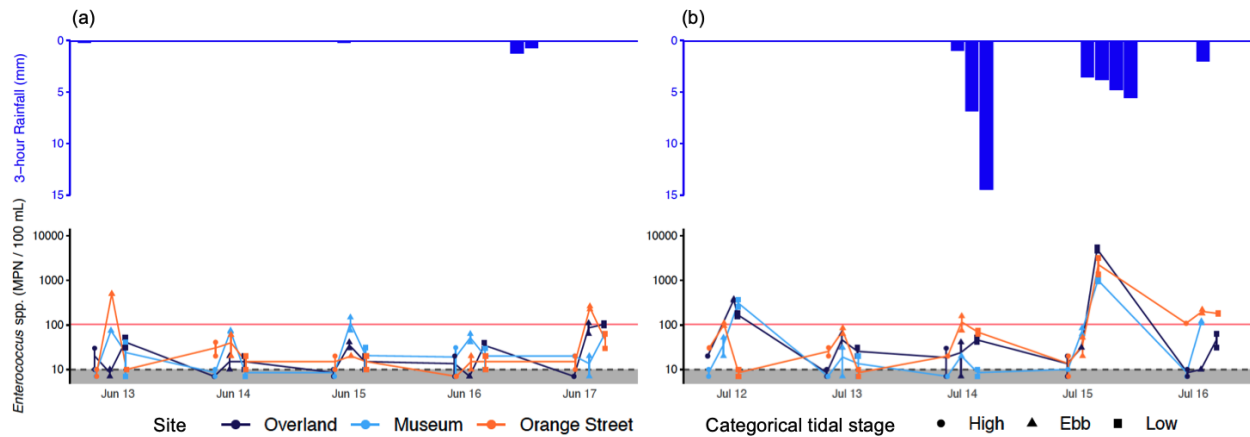436   both the June and July events.

437

Figure 5. 3-hour rainfall (top) and ENT concentrations (bottom) from Taylor's Creek during
perigean tide events from June 12-17, 2022 (**a**) and July 11-16, 2022 (**b**). The red line represents
the EPA's single sample maximum threshold concentration for safe public use (104 MPN 100
mL^{-1}), and the grayed area represents the minimum detection limit (below 10 MPN 100 mL^{-1} for
samples diluted 10:1). Point shapes correspond to the tidal stages of high, ebb, and low, while the
colors correspond to sampling locations.

444   Although the highest ENT concentrations in the waterway during the perigean tide events
445   were observed during ebb and low tide, the majority of concentrations were below the EPA's
446   threshold for safe public use, demonstrating that the observed conditions did not pose a public
447   health hazard. Yet, the observed increase in ENT concentrations during ebb tide in a large and
448   dynamic waterway like Taylor's Creek demonstrates that tidal floods and stormwater network
449   inundation can serve as a source of fecal contamination to surface waters and are worthy of
450   further investigation as an emerging public health concern, particularly in coastal communities
451   that drain to relatively small tidal creeks with minimal potential to flush or dilute pollutants.

452   From the results of our robust linear mixed effect models for the perigean tides (**Table 1**),
453   tidal height at sample collection and time to last high tide were associated with the greatest and
454   second greatest marginal R^2 values (0.20 and 0.13, respectively). Though they cannot explain the
455   majority of ENT variance (i.e., they do not have marginal $R^2 > 0.5$), the marginal R^2 values of
456   tidal height at sample collection and time to last high tide support prior recommendations by
457   Price et al. (2021) that tidal variables be included and documented as part of coastal ENT
458   monitoring efforts, as tidal effects can play a role in transporting ENT within coastal systems.

459   For perigean tide conditions, height of the last high tide and rainfall variables had low
460   marginal R^2 values and coefficients that were not significantly different from zero (**Table 1**).
461   Because height of last high tide was not a significant descriptor of ENT concentration variance,
462   we conclude that maximum inundation prior to sampling was not the most important factor
463   explaining the elevated ENT concentrations during ebb tide for our study site. However, height
464   of last high tide should not be discounted as a potential variable to monitor, as other coastal
465   stormwater network configurations may exhibit increase in ENT concentrations with higher tidal
466   heights. Likewise, our results do not necessarily indicate that rainfall is not an important
467   descriptor to ENT variability during the ebb tide and drainage of the stormwater network, as
468   other studies have demonstrated a direct link between rainfall and ENT concentration in coastal
469   waterways (Mallin et al., 2000). The low marginal R^2 values of our tested rainfall variables is
470   likely from our sampling design which targeted the tidal dynamics of the 6-7 hour period
471   between the higher high tide and the higher low tide, and from the paucity of rainfall events that
472   occurred during our sampling window.

473   3.5 Stormwater runoff drives higher ENT concentrations than tidal inundation

474   During baseline conditions, stormwater runoff drove higher ENT concentrations in the
475   waterway than tidal inundation. Many studies have reported increased FIB concentrations in
476   waterways following rainfall events (Converse et al., 2011; Gonzalez et al., 2012; Parker et al.,
477   2010; Stumpf et al., 2010), and our results support this finding for baseline conditions (i.e., when
478   there is no roadway flooding from complete stormwater inundation by tides). Prior rainfall totals
479   were significantly related to daily ENT variance in the waterway during baseline conditions
480   (**Table 1**). Specifically, antecedent rainfall over 3, 6, 12, 24, 48, and 72 hours prior to sample
481   collection had larger marginal R^2 values (0.10-0.35) in the baseline model than the significant
482   tidal variables (0.04-0.06). While antecedent rainfall predominantly explained the baseline ENT
483   concentrations, rain variables did not significantly explain ENT variance during perigean tides,
484   as discussed above. However, we observed that recent rainfall events coincided with the
485   maximum ENT concentrations observed in Taylor's Creek during the perigean tide periods (Fig
486   5). Low tide samples collected on July 15, 2022, which coincided with a compound flood event

487 (rainfall plus reduced capacity in the stormwater network due to tidal inundation), displayed the
488 maximum ENT concentrations observed in the waterway during both perigean tides. These
489 samples were collected 20 hours after a 22-mm, 8-hour rainfall event occurred the previous day,
490 and during the first hour of a 17-mm rainstorm that lasted over 9 hours. Approximately 3.6 mm
491 of rainfall occurred during the first hour of the event.

492 **4 Conclusions**

493 Our findings indicate that chronic stormwater network inundation and tidal flooding
494 caused by SLR present pathways for fecal contamination of coastal surface waters and roadway
495 floodwaters, but research is needed to fully understand whether network inundation and floods
496 create public health hazards. In this study, we consistently observed high ENT concentrations
497 above the US EPA's single sample maximum threshold for safe public use of recreational waters
498 in tidal and compound floodwaters on a roadway in Beaufort, NC. These measurements were
499 taken from minor floods with minimal overland footprints, leading us to believe the sources of
500 the elevated ENT in the floodwaters were within the stormwater network and could include
501 undrained stormwater runoff, pipe biofilms and sediment, and exfiltrated sewage. However, we
502 did not observe similarly concerning ENT concentrations in Taylor's Creek, the adjacent coastal
503 waterway, as a function of tide-driven stormwater network inundation. Rainfall-driven runoff
504 produced higher ENT concentrations in Taylor's Creek than stormwater network inundation and
505 tidal flooding, reinforcing that stormwater runoff is the dominant driver of increased ENT
506 concentrations in the coastal waterway. However, we observed short-lived increases in ENT
507 concentrations in Taylor's Creek as perigean tides receded from the stormwater network, and we
508 hypothesize the temporary increase in ENT concentrations is due to dilution or flushing given
509 that Taylor's Creek is a large coastal waterway. In relatively small tidal creeks draining urban
510 centers, the effects of dilution and flushing may not be as apparent, and the role of stormwater
511 network inundation and tidal flooding on ENT concentrations may be more pronounced.

512 This study provided needed longitudinal water quality observations across a two-month
513 period that included nine tidal floods from two perigean tide events, which allowed us to assess
514 potential public health hazards from tidal flooding and make inferences on the relative roles of
515 stormwater network inundation, tidal flooding, and rain on fecal contamination both in a coastal
516 waterway and roadway floodwaters. However, the small size of the tidal floods we observed
517 prevents us from concluding whether more extensive floods are associated with higher or lower
518 ENT concentrations. Additionally, while our results demonstrate that tidal floods are associated
519 with problematic water quality in both roadway floodwaters and coastal surface waters as was
520 shown in previous studies (Macías-Tapia et al., 2021, 2023; Hart et al., 2020; Price et al., 2021;
521 McKenzie et al., 2021), similar studies as the one presented here should be conducted across
522 more locations to better understand site-specific effects related to stormwater infrastructure and
523 land use. We suggest that future work incorporate sampling across multiple seasons,
524 communities, and flood extents to better understand the prevalence of poor water quality from
525 chronic stormwater network inundation and tidal flooding. Seasonal differences may contribute
526 to the persistence of ENT within the stormwater network, while community differences in
527 infrastructure, topography, land use, and waterway size could contribute to the type and number
528 of ENT sources as well as the effect of tidal flushing on ENT concentrations in the waterway.

529   Ultimately, the water quality effects of chronic stormwater network inundation and tidal
530 flooding are evolving given the non-stationarity of global climate change and SLR. SLR brings
531 uncertainty to whether tidally-driven inundation and associated pollutant loading will remain at
532 their current levels, as the magnitude of the loading will likely change with increased flooding
533 frequency and damage to infrastructure. For Beaufort and other cities on the Atlantic coast of the
534 US, rates of SLR are 30% higher than the global average of 3 mm/year (Ezer & Atkinson, 2014),
535 meaning that future repetition of this study could produce differing results as tidally-driven
536 inundation becomes more intense and widespread.

Acknowledgments

Open Research

545 All data and R code are provided as supporting materials with the manuscript for peer review
546 purposes. Following review, the data and code will be archived with Dryad and a permanent DOI
547 will be included in this section.

References

549 Allen, T. R., Crawford, T., Montz, B., Whitehead, J., Lovelace, S., Hanks, A. D., Christensen, A.
550   R., & Kearney, G. D. (2019). Linking Water Infrastructure, Public Health, and Sea Level
551   Rise: Integrated Assessment of Flood Resilience in Coastal Cities. *Public Works*
552   *Management & Policy*, *24*(1), 110–139. https://doi.org/10.1177/1087724X18798380

553 Befus, K. M., Kurnizki, A. P. D., Kroeger, K. D., Eagle, M. J., & Smith, T. P. (2023).
554   Forecasting Sea Level Rise-driven Inundation in Diked and Tidally Restricted Coastal
555   Lowlands. *Estuaries and Coasts*, *46*(5), 1157–1169. https://doi.org/10.1007/s12237-023-
556   01174-1

557 Boehm, A. B. (2007). Enterococci Concentrations in Diverse Coastal Environments Exhibit
558   Extreme Variability. *Environmental Science & Technology*, *41*(24), 8227–8232.
559   https://doi.org/10.1021/es071807v

560 Burkhart, T. H. (Tsung H. S. (2013). *Biofilms as sources of fecal bacteria contamination in the*
561   *stormwater drainage system in Singapore* [Thesis, Massachusetts Institute of
562   Technology]. https://dspace.mit.edu/handle/1721.1/82805

563 Center for Operational Oceanographic Products and Services. (2022). Tide & Currents for
564   Beaufort, Duke Marine Lab, NC - Station ID: 8656483. National Oceanic and
565   Atmospheric Administration.
566   https://tidesandcurrents.noaa.gov/stationhome.html?id=8656483

567 Converse, R. R., Piehler, M. F., & Noble, R. T. (2011). Contrasts in concentrations and loads of
568   conventional and alternative indicators of fecal contamination in coastal stormwater.
569   *Water Research*, *45*(16), 5229–5240. https://doi.org/10.1016/j.watres.2011.07.029

570 Division of Water Resources. (2023, March). *2022 North Carolina 303(d) List*. North Carolina
571   Department of Environmental Quality.
572   https://edocs.deq.nc.gov/WaterResources/DocView.aspx?dbid=0&id=2738821

573 Ezer, T., & Atkinson, L. P. (2014). Accelerated flooding along the U.S. East Coast: On the
574   impact of sea-level rise, tides, storms, the Gulf Stream, and the North Atlantic
575   Oscillations. *Earth's Future*, *2*(8), 362–382. https://doi.org/10.1002/2014EF000252

576 Gold, A., Anarde, K., Grimley, L., Neve, R., Srebnik, E. R., Thelen, T., Whipple, A., & Hino, M.
577   (2023). Data From the Drain: A Sensor Framework That Captures Multiple Drivers of
578   Chronic Coastal Floods. *Water Resources Research*, *59*(4), e2022WR032392.
579   https://doi.org/10.1029/2022WR032392

580 Gold, A. C., Brown, C. M., Thompson, S. P., & Piehler, M. F. (2022). Inundation of Stormwater
581   Infrastructure Is Common and Increases Risk of Flooding in Coastal Urban Areas Along
582   the US Atlantic Coast. *Earth's Future*, *10*(3), e2021EF002139.
583   https://doi.org/10.1029/2021EF002139

584 Gonzalez, R. A., Conn, K. E., Crosswell, J. R., & Noble, R. T. (2012). Application of empirical
585   predictive modeling using conventional and alternative fecal indicator bacteria in eastern
586   North Carolina waters. *Water Research*, *46*(18), 5871–5882.
587   https://doi.org/10.1016/j.watres.2012.07.050

588 Habel, S., Fletcher, C. H., Anderson, T. R., & Thompson, P. R. (2020). Sea-Level Rise Induced
589   Multi-Mechanism Flooding and Contribution to Urban Infrastructure Failure. *Scientific*
590   *Reports*, *10*, 3796. https://doi.org/10.1038/s41598-020-60762-4

591 Hart, J. D., Blackwood, A. D., & Noble, R. T. (2020). Examining coastal dynamics and
592   recreational water quality by quantifying multiple sewage specific markers in a North
593   Carolina estuary. *Science of The Total Environment*, *747*, 141124.
594   https://doi.org/10.1016/j.scitotenv.2020.141124

595   Health and Ecological Criteria Division, Office of Science and Technology. (2012,
596   December). Recreational Water Quality Criteria. (EPA-820-F-12-061). Environmental
597   Protection Agency. Office of Water. https://www.epa.gov/sites/default/files/2015-
598   10/documents/rwqc2012.pdf

599 IDEXX. (2019, May). Standard Test Method for Enterococci in Water Using Enterolert. (ASTM
600   D6503-19). IDEXX. https://www.astm.org/d6503-19.html

601 Koller, M. (2016). robustlmm: An R Package for Robust Estimation of Linear Mixed-Effects
602   Models. *Journal of Statistical Software*, *75*, 1–24. https://doi.org/10.18637/jss.v075.i06

603 Lewis, D. J., Atwill, E. R., Pereira, M. das G. C., & Bond, R. (2013). Spatial and Temporal
604   Dynamics of Fecal Coliform and Escherichia coli Associated with Suspended Solids and

605   Water within Five Northern California Estuaries. *Journal of Environmental Quality*,
606   *42*(1), 229–238. https://doi.org/10.2134/jeq2011.0479

607 Lüdecke, D., Ben-Shachar, M., Patil, I., & Makowski, D. (2020). Extracting, Computing and
608   Exploring the Parameters of Statistical Models using R. *Journal of Open Source*
609   *Software*, *5*(53), 2445. https://doi.org/10.21105/joss.02445

610 Lüdecke, D., Ben-Shachar, M. S., Patil, I., Waggoner, P., & Makowski, D. (2021). performance:
611   An R Package for Assessment, Comparison and Testing of Statistical Models. *Journal of*
612   *Open Source Software*, *6*(60), 3139. https://doi.org/10.21105/joss.03139

613 Macías-Tapia, A., Mulholland, M. R., Selden, C. R., Loftis, J. D., & Bernhardt, P. W. (2021).
614   Effects of tidal flooding on estuarine biogeochemistry: Quantifying flood-driven nitrogen
615   inputs in an urban, lower Chesapeake Bay sub-tributary. *Water Research*, *201*, 117329.
616   https://doi.org/10.1016/j.watres.2021.117329

617 Macías-Tapia, A., Mulholland, M. R., Selden, C. R., Loftis, J. D., & Bernhardt, P. W. (2023).
618   Five Years Measuring the Muck: Evaluating Interannual Variability of Nutrient Loads
619   From Tidal Flooding. *Estuaries and Coasts*, *46*(7), 1756–1776.
620   https://doi.org/10.1007/s12237-023-01245-3

621 Mallin, M. A., Williams, K. E., Esham, E. C., & Lowe, R. P. (2000). Effect of Human
622   Development on Bacteriological Water Quality in Coastal Watersheds. *Ecological*
623   *Applications*, *10*(4), 1047–1056. https://doi.org/10.1890/1051-
624   0761(2000)010[1047:EOHDOB]2.0.CO;2

625 McKenzie, T., Habel, S., & Dulai, H. (2021). Sea-level rise drives wastewater leakage to coastal
626   waters and storm drains. *Limnology and Oceanography Letters*, *6*(3), 154–163.
627   https://doi.org/10.1002/lol2.10186

628 Olds, H. T., Corsi, S. R., Dila, D. K., Halmo, K. M., Bootsma, M. J., & McLellan, S. L. (2018).
629   High levels of sewage contamination released from urban areas after storm events: A
630   quantitative survey with sewage specific bacterial indicators. *PLoS Medicine*, *15*(7),
631   e1002614. https://doi.org/10.1371/journal.pmed.1002614

632 Parker, J. K., McIntyre, D., & Noble, R. T. (2010). Characterizing fecal contamination in
633   stormwater runoff in coastal North Carolina, USA. *Water Research*, *44*(14), 4186–4194.
634   https://doi.org/10.1016/j.watres.2010.05.018

635 Price, M. T., Blackwood, A. D., & Noble, R. T. (2021). Integrating culture and molecular
636   quantification of microbial contaminants into a predictive modeling framework in a low-
637   lying, tidally-influenced coastal watershed. *Science of The Total Environment*, *792*,
638   148232. https://doi.org/10.1016/j.scitotenv.2021.148232

639 R Core Team (2013). R: A language and environment for statistical computing. R Foundation for
640   Statistical Computing, Vienna, Austria. ISBN 3-900051-07-0, URL http://www.R-
641   project.org/

642 Sercu, B., Van De Werfhorst, L. C., Murray, J. L., & Holden, P. A. (2011). Sewage exfiltration

643   as a source of storm drain contamination during dry weather in urban watersheds.
644   *Environmental science & technology*, *45*(17), 7151-7157.

645 State Climate Office of North Carolina. (2022) *Michael J Smith Field Airport (KMRH) hourly*
646   *and daily rainfall, June-August 2022* [Data set]. NOAA National Weather Service.
647   https://products.climate.ncsu.edu/data/

648 Strauss, B. H., Ziemlinski, R., Weiss, J. L., & Overpeck, J. T. (2012). Tidally adjusted estimates
649   of topographic vulnerability to sea level rise and flooding for the contiguous United
650   States. *Environmental Research Letters*, *7*(1), 014033. https://doi.org/10.1088/1748-
651   9326/7/1/014033

652 Stumpf, C. H., Piehler, M. F., Thompson, S., & Noble, R. T. (2010). Loading of fecal indicator
653   bacteria in North Carolina tidal creek headwaters: Hydrographic patterns and terrestrial
654   runoff relationships. *Water Research*, *44*(16), 4704–4715.
655   https://doi.org/10.1016/j.watres.2010.07.004

656 Sweet, W., Hamlington, B.D., Kopp, R. E., & Zuzak, C. (2022). *Global and Regional Sea Level*
657   *Rise Scenarios for the United States: Updated Mean Projections and Extreme Water*
658   *Level Probabilities Along U.S. Coastlines* (p. 111) [Technical Report]. National Oceanic
659   and Atmospheric Administration.
660   https://aambpublicoceanservice.blob.core.windows.net/oceanserviceprod/hazards/sealeve
661   lrise/noaa-nos-techrpt01-global-regional-SLR-scenarios-US.pdf

662 University of North Carolina - Chapel Hill. (2022). *2022 King Tides Calendar*. North Carolina
663   King Tides Project. https://nckingtides.web.unc.edu/